Supplementary Table 1. Clinical characteristics of chordoid glioma patient cohort.

Patient	Age at dx	Sex	Presenting symptoms	Treatment	Outcome
CG-UCSF-1	45	F	headache and nausea	subtotal resection, external beam radiation	died of disease 7 months after dx
CG-UCSF-2	65	F	cognitive decline	biopsy, external beam radiation	died of disease 14 months after dx
CG-UCLA-1	34	M	hypogonadism	biopsy, external beam radiation	alive with stable disease at 53 months after dx
CG-UVA-1	48	M	unknown	subtotal resection	unknown
CG-UVA-2	47	M	unknown	subtotal resection	died of post-operative complications one week after dx
CG-JHH-1	34	M	unknown	resection	unknown
CG-MSK-1	57	F	none, incidentally found	gross total resection	alive with no evidence of disease at 13 years after dx
CG-MSK-2	37	F	unknown	resection	unknown
CG-UCO-1	67	M	hypothermia and dysequilibrium	biopsy followed by subtotal resection	alive with stable disease at 2 months after dx
CG-MGH-1	53	F	unknown	resection	unknown
CG-NYU-1	45	F	somnolence and cognitive decline	subtotal resection	unknown
CG-Egypt-1	49	F	somnolence and headaches	biopsy	unknown
CG-Brazil-1	58	M	unknown	resection	unknown

Supplementary Table 2. Somatic *PRKCA* mutations identified in the 13 chordoid gliomas.

Tumor	Chromosome	Position	Reference allele	Variant allele	Gene	Variant	Variant	Reference transcript	Tumor coverage	Tumor mutant allele frequency	Normal coverage	Normal mutant allele frequency
CG-UCSF-1	chr17	64738741	G	C	PRKCA	c.1387G>C	p.D463H	NM_002737	212	41%	212	0%
CG-UCSF-2	chr17	64738741	G	C	PRKCA	c.1387G>C	p.D463H	NM_002737	458	19%	-	-
CG-UCLA-1	chr17	64738741	G	C	PRKCA	c.1387G>C	p.D463H	NM_002737	282	35%	106	0%
CG-UVA-1	chr17	64738741	G	C	PRKCA	c.1387G>C	p.D463H	NM_002737	52	22%	-	-
CG-UVA-2	chr17	64738741	G	C	PRKCA	c.1387G>C	p.D463H	NM_002737	144	22%	-	-
CG-JHH-1	chr17	64738741	G	C	PRKCA	c.1387G>C	p.D463H	NM_002737	406	21%	-	-
CG-MSK-1	chr17	64738741	G	C	PRKCA	c.1387G>C	p.D463H	NM_002737	95	42%	-	-
CG-MSK-2	chr17	64738741	G	C	PRKCA	c.1387G>C	p.D463H	NM_002737	273	34%	-	-
CG-UCO-1	chr17	64738741	G	C	PRKCA	c.1387G>C	p.D463H	NM_002737	556	21%	-	-
CG-MGH-1	chr17	64738741	G	C	PRKCA	c.1387G>C	p.D463H	NM_002737	158	31%	-	-
CG-NYU-1	chr17	64738741	G	C	PRKCA	c.1387G>C	p.D463H	NM_002737	448	13%	-	-
CG-Egypt-1	chr17	64738741	G	C	PRKCA	c.1387G>C	p.D463H	NM_002737	59	12%	-	-
CG-Brazil-1	chr17	64738741	G	C	PRKCA	c.1387G>C	p.D463H	NM_002737	443	21%	-	-

Supplementary Table 3. Chromosomal copy number alterations identified in the 13 chordoid gliomas.

Tumor	Gains	Losses
CG-UCSF-1	1q, 8	6q
CG-UCSF-2	none	none
CG-UCLA-1	none	none
CG-UVA-1	none	none
CG-UVA-2	none	none
CG-JHH-1	none	none
CG-MSK-1	none	18
CG-MSK-2	none	1p
CG-UCO-1	none	none
CG-MGH-1	none	none
CG-NYU-1	none	none
CG-Egypt-1	none	none
CG-Brazil-1	none	none

CG-UCSF-1

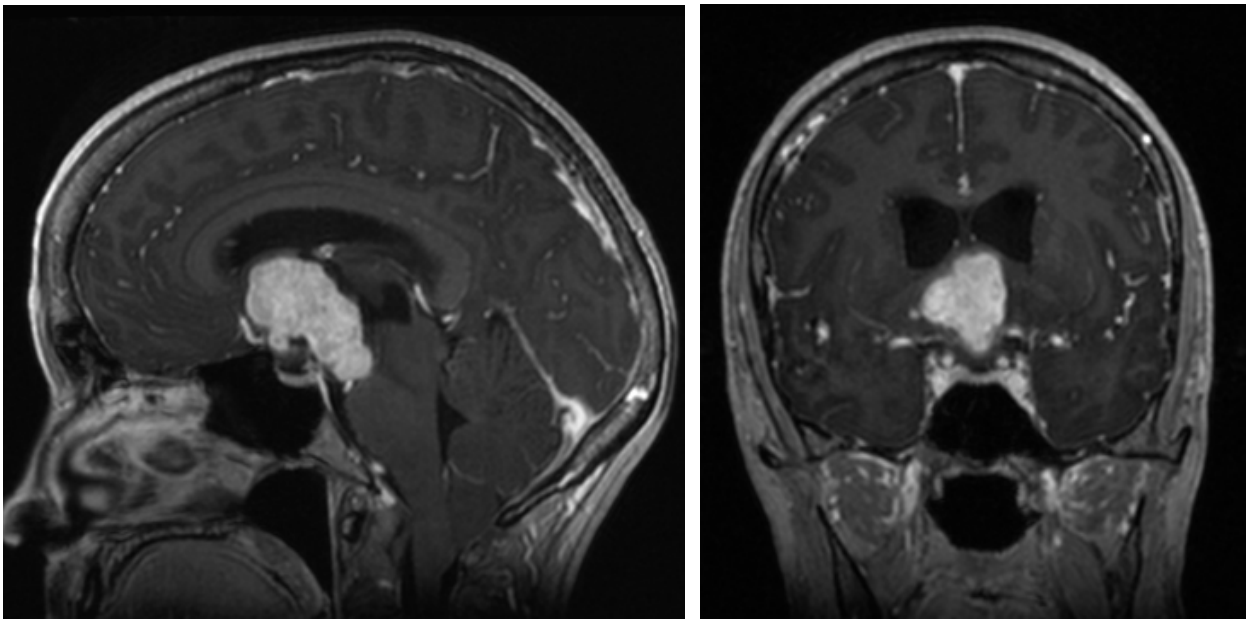

CG-UCSF-2

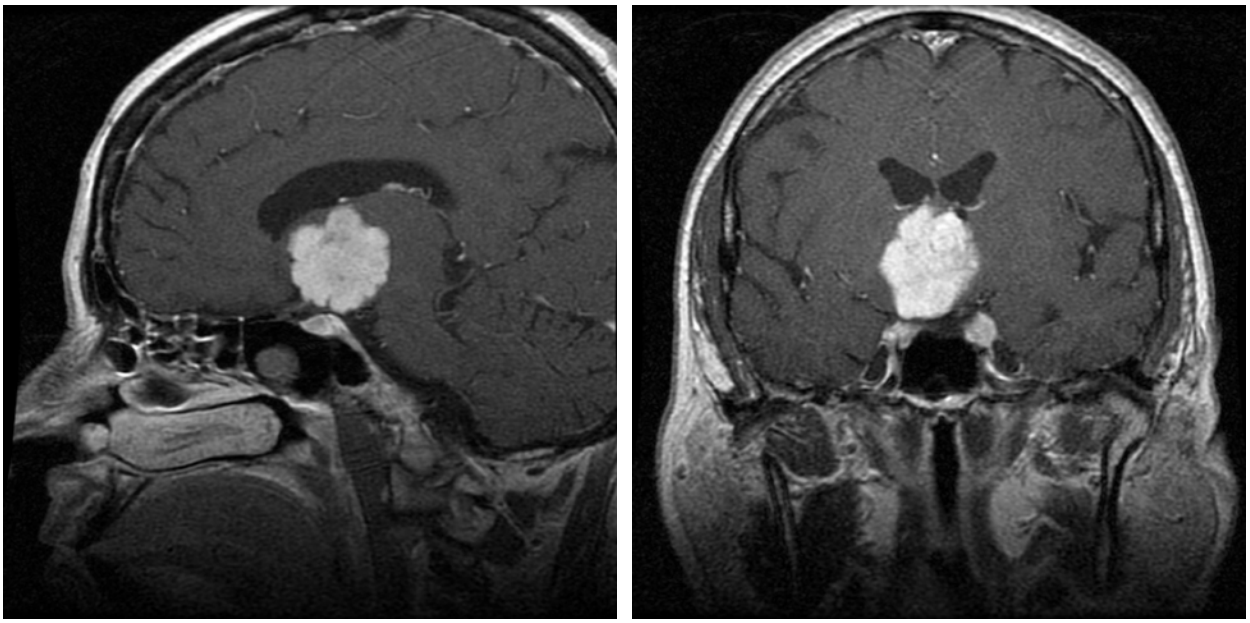

CG-UCO-1

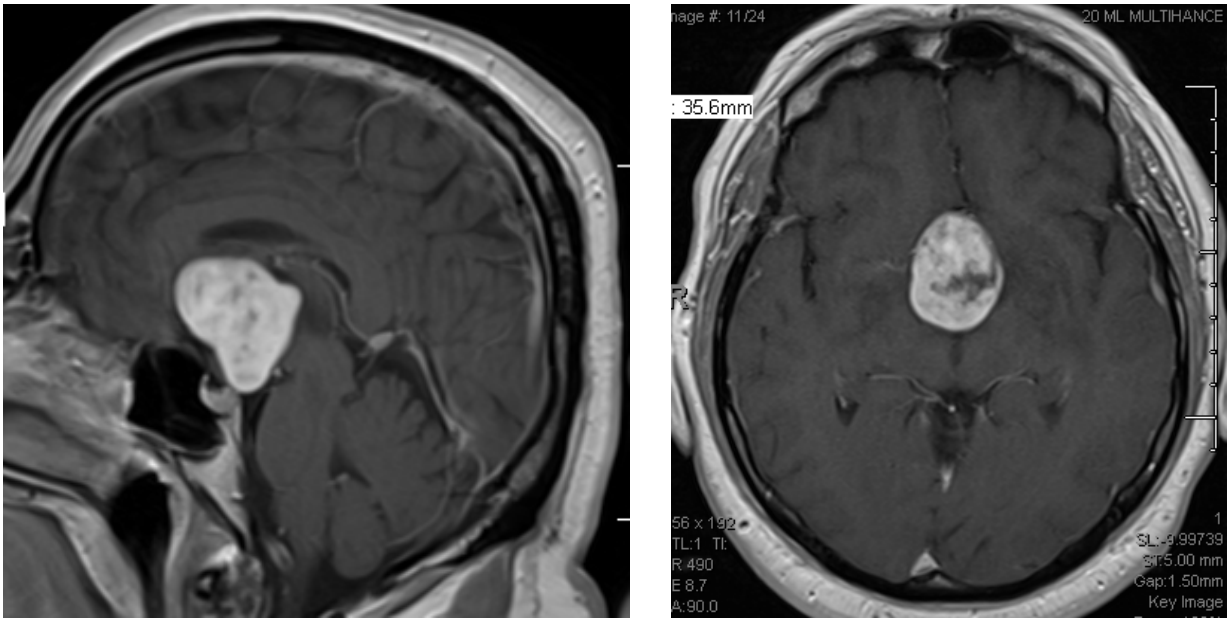

Supplementary Figure 1. Radiographic features of the chordoid gliomas. Shown are T1-weighted post-contrast magnetic resonance images demonstrating enhancing, well-circumscribed masses centered in the anterior third ventricle in all cases.

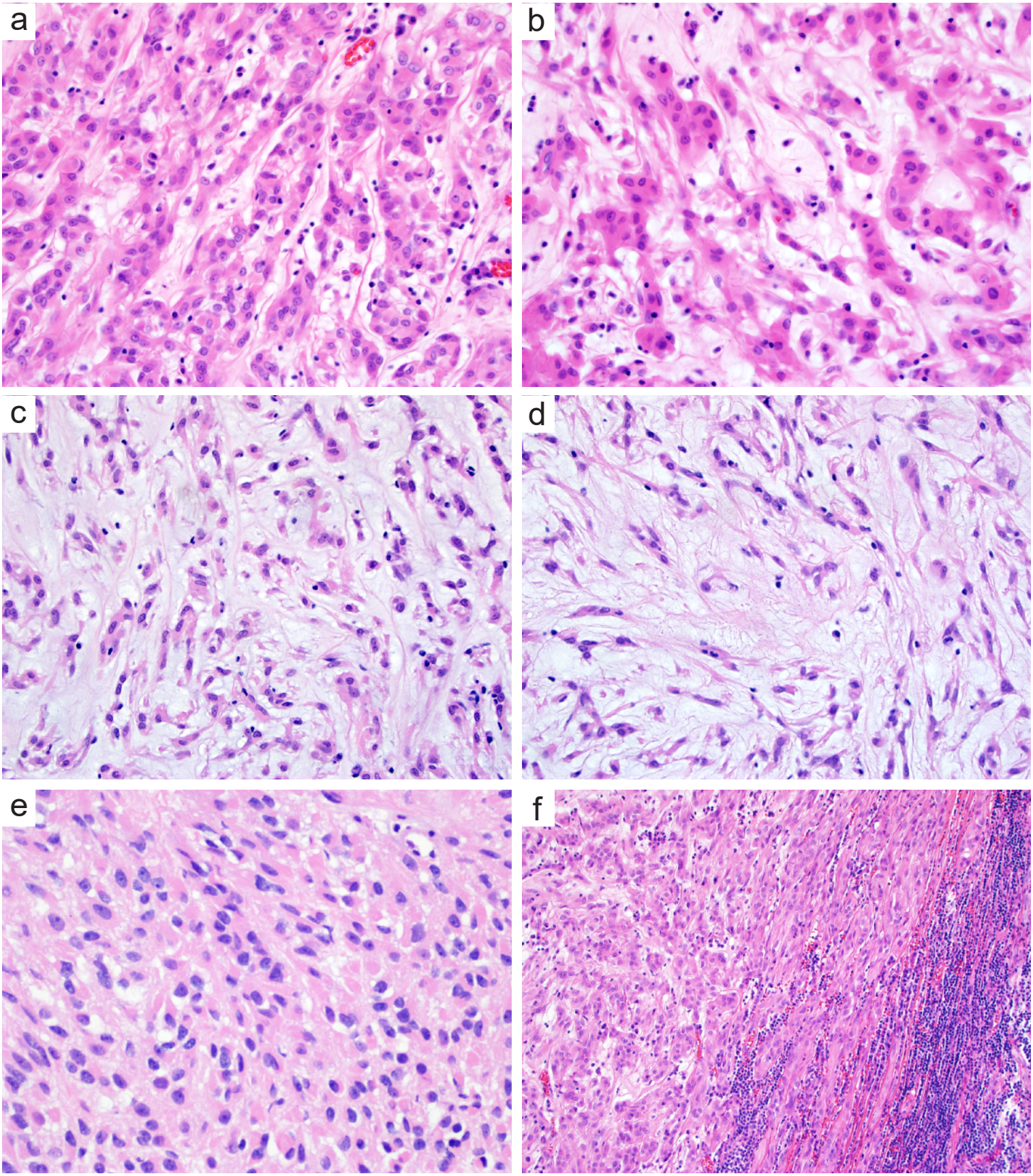

Supplementary Figure 2. Histologic features of the chordoid gliomas. (**a,b**) Tumors are characterized by cohesive cords and clusters of epithelioid cells with abundant eosinophilic cytoplasm in a mucin-rich stroma. Mitotic activity and nuclear atypia are minimal (CG-UVA-1). (**c,d**) Some tumors demonstrate more elongate to spindled morphology (CG-UCO-1). (**e**) Some tumors contain solid areas reminiscent of subependymal giant cell astrocytoma (CG-UCSF-1). (**f**) A common feature is the presence of a dense lymphoplasmacytic inflammatory infiltrate, often at the periphery of the tumor (CG-UVA-1).

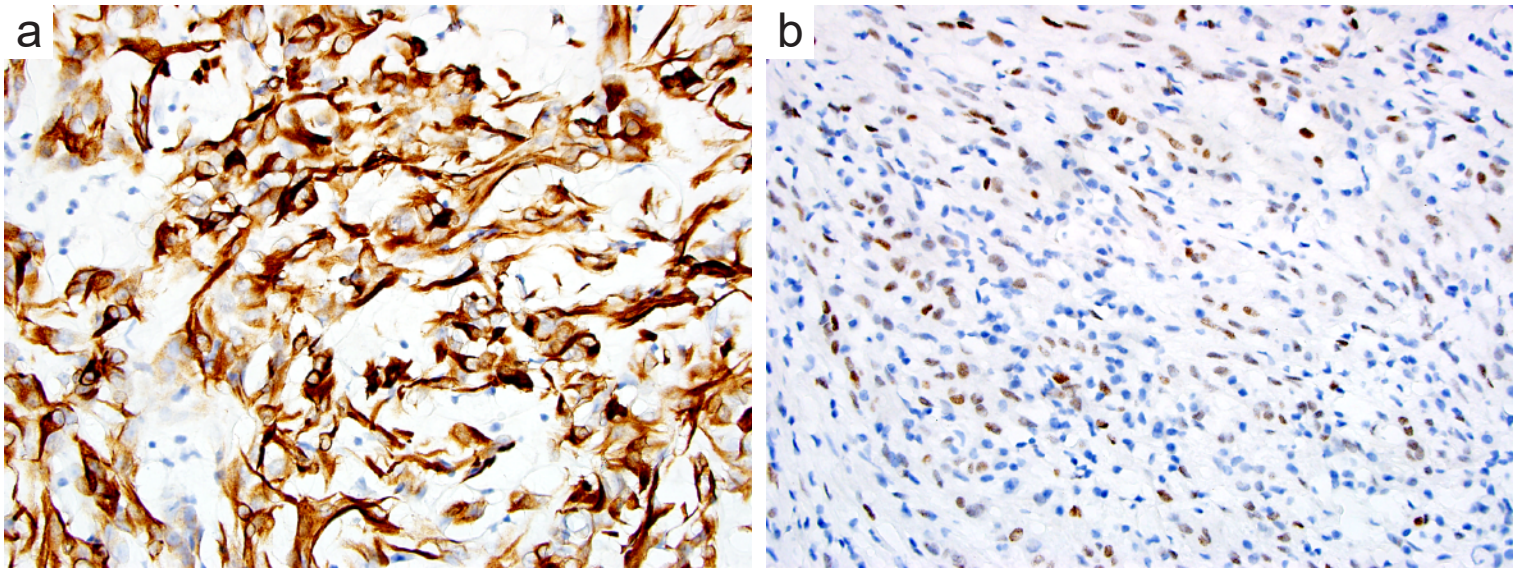

Supplementary Figure 3. Immunohistochemical features of the chordoid gliomas. (**a**) Diffuse positivity for glial fibrillary acidic protein (GFAP) in tumor cells. (**b**) Nuclear positivity for TTF-1 (also known as NKX2.1) in a subset of tumor cells.

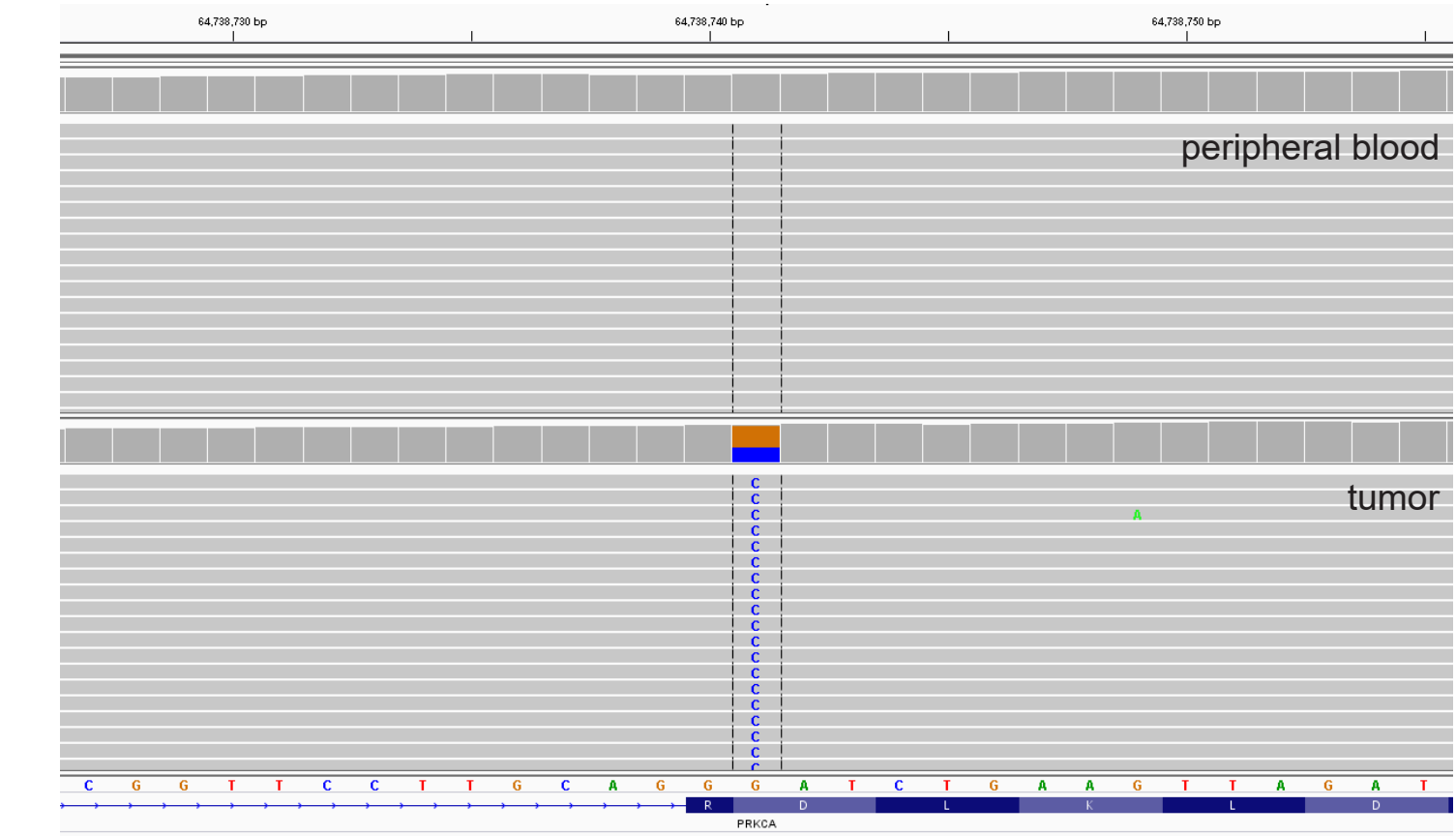

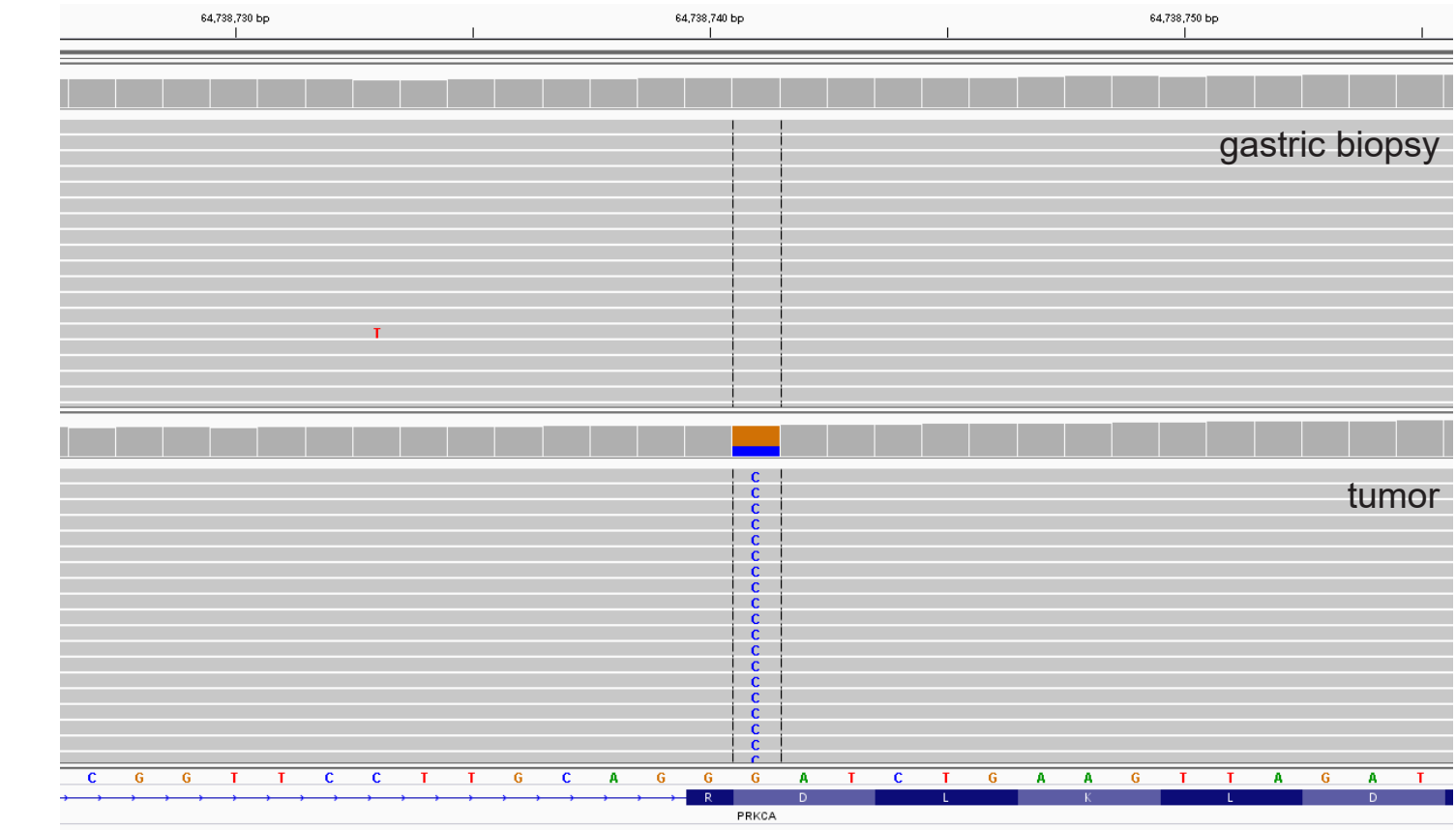

Supplementary Figure 4. A recurrent somatic *PRKCA* p.D463H mutation defines chordoid glioma of the third ventricle. Sequencing reads containing a G>C mutation in two tumor samples but not in matched normal tissue from the patients causing a p.D463H substitution. (**a**) Tumor CG-UCSF-1. (**b**) Tumor CG-UCLA-1.

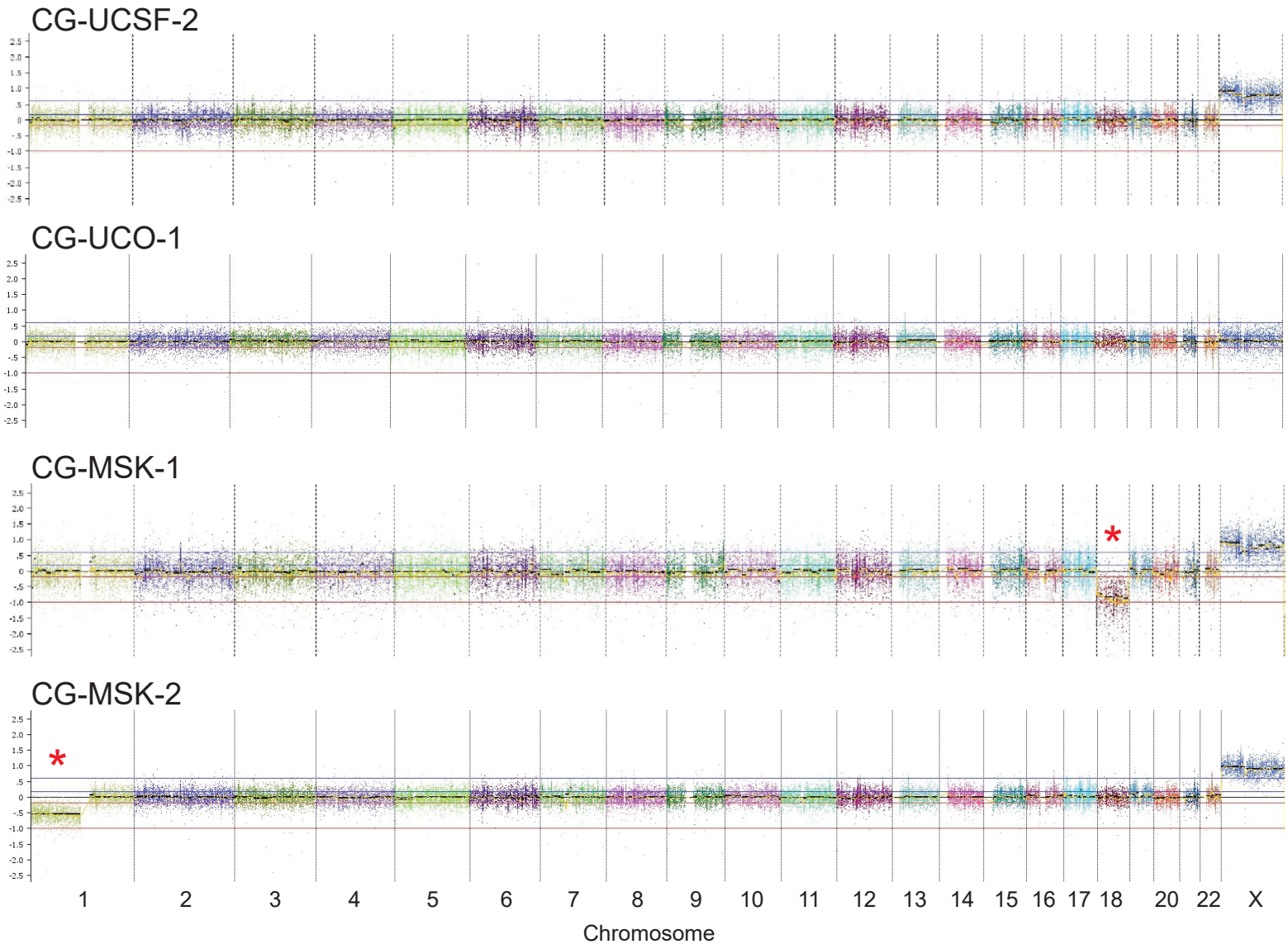

Supplementary Figure 5. Chromosomal copy number alterations in the 13 chordoid gliomas. Genome-wide copy number inferred from targeted next-generation sequencing data revealed a balanced diploid genome in 10 of the tumors including CG-UCSF-2 and CG-UCO-1. Tumor CG-MSK-1 demonstrated loss of chromosome 18. Tumor CG-MSK-2 demonstrated loss of chromosome 1p. Tumor CG-UCSF-1 demonstrated loss of chromosome 6q and gains of 1p and 8. No focal amplifications or deletions were identified in any of the tumors.

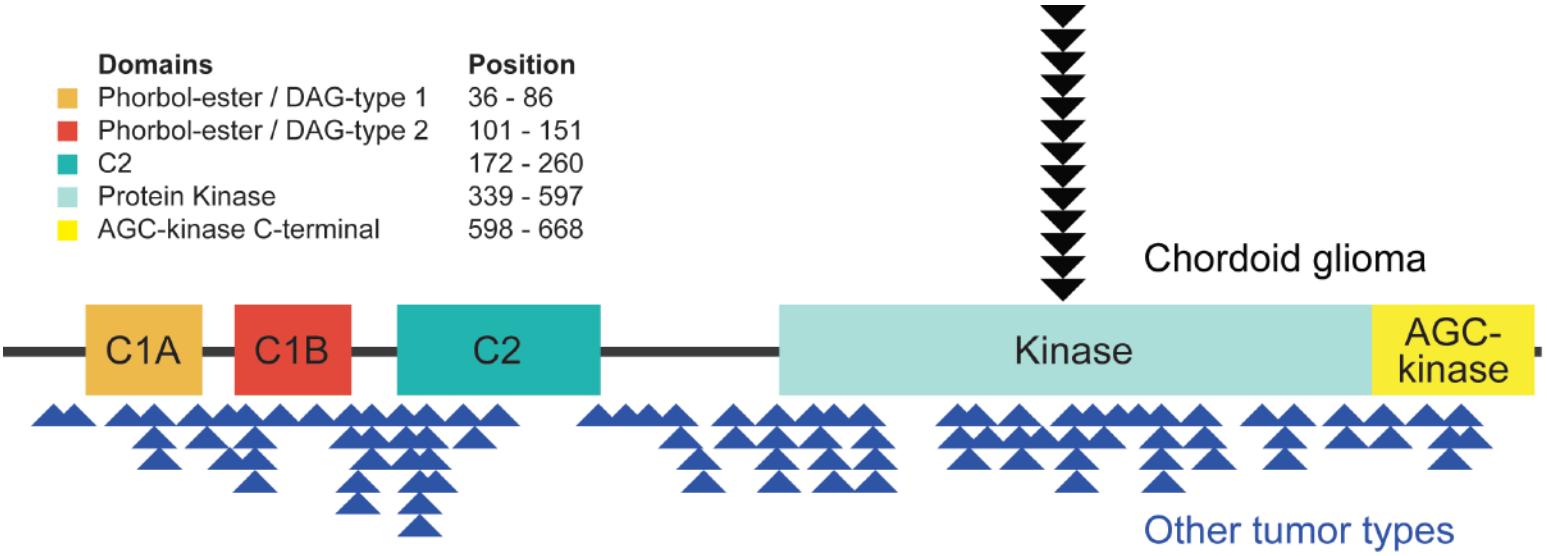

Tumor Type	Non-synonymous somatic mutations
Adrenal gland	0 / 613 (0.0%)
Autonomic ganglia	0 / 766 (0.0%)
Biliary tract	1 / 368 (0.3%)
Bone	1 / 567 (0.2%)
Breast	9 / 2327 (0.4%)
Cervix	3 / 324 (0.9%)
Endometrium	0 / 640 (0.0%)
Esophagus	1 / 1105 (0.1%)
Hematopoietic	1 / 3380 (0.0%)
Kidney	2 / 1742 (0.1%)
Large intestine	12 / 1594 (0.8%)
Liver	3 / 1816 (0.2%)
Lung	3 / 2283 (0.1%)
Oropharynx	4 / 1238 (0.3%)
Ovary	3 / 925 (0.3%)
Pancreas	5 / 1766 (0.3%)
Pleura	0 / 164 (0.0%)
Prostate	4 / 1563 (0.3%)
Skin	26 / 1215 (2.1%)
Soft tissue	1 / 542 (0.2%)
Stomach	7 / 824 (0.8%)
Thyroid	0 / 697 (0.0%)
Urinary tract	1 / 672 (0.1%)

CNS Tumor Type	Non-synonymous somatic mutations
Diffuse/anaplastic astrocytoma	0 / 107 (0.0%)
Oligodendroglioma	0 / 37 (0.0%)
Glioblastoma	1 / 929 (0.1%)
Glioma NOS	2 / 609 (0.3%)
Pilocytic astrocytoma	0 / 10 (0.0%)
Pleomorphic xanthoastrocytoma	0 / 12 (0.0%)
Ependymoma	0 / 55 (0.0%)
Medulloblastoma	1 / 499 (0.2%)
Atypical teratoid/rhabdoid tumor	0 / 23 (0.0%)

Supplementary Figure 6. Domain structure of the human PKCα protein with the location of the p.D463H mutation identified in each of the 13 chordoid gliomas (black arrowheads). Also shown are all confirmed somatic nonsynonymous mutations in the 30,367 human tumors with *PRKCA* sequencing data available in the version 81 release of the Catalogue of Somatic Mutations in Cancer (COSMIC) database (blue arrowheads).

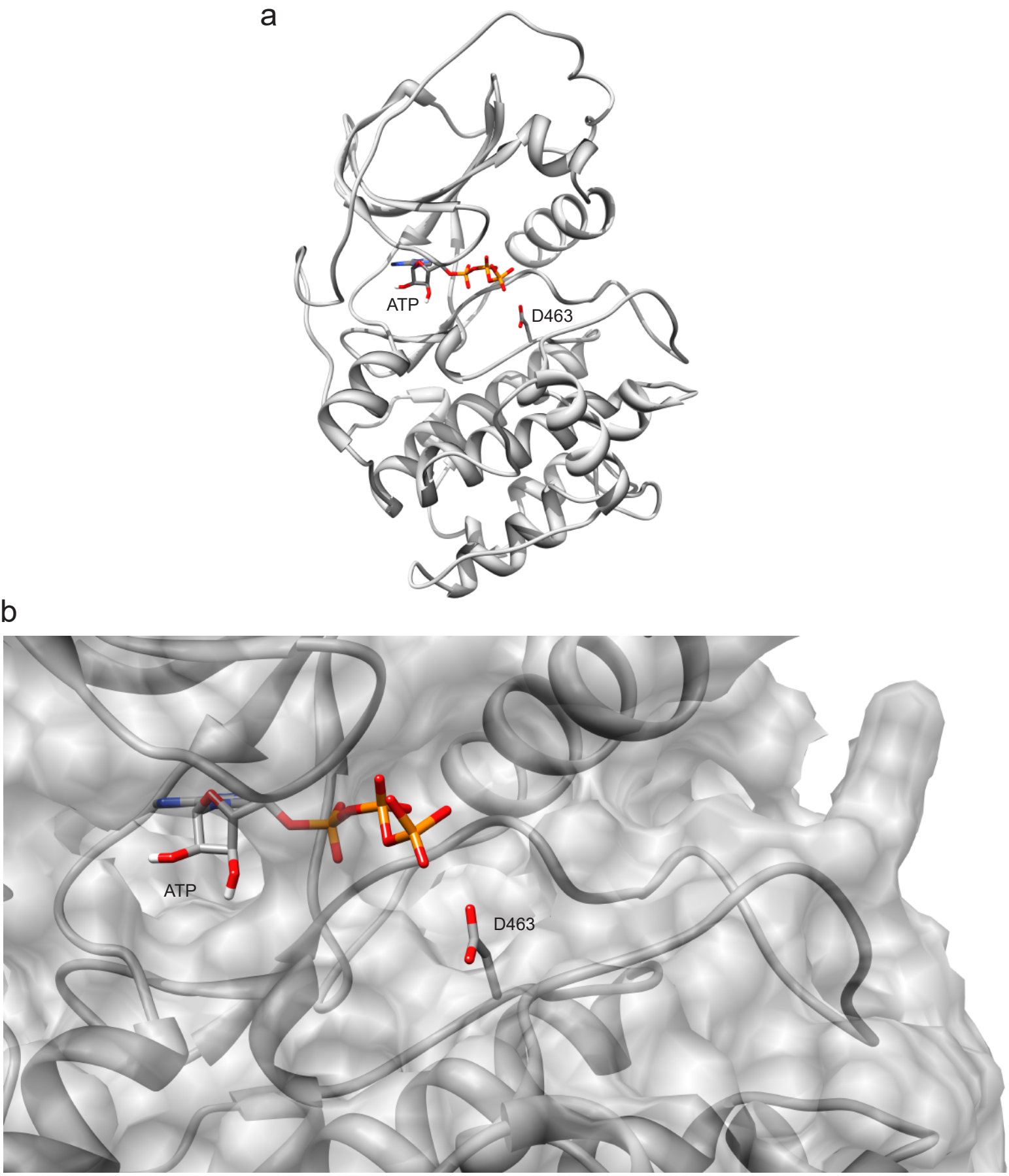

Supplementary Figure 7. Structural modeling of wildtype and D463H-mutant PKCα. (**a**) Model of PKCα with wildtype p.D463 (Asp463) and ATP bound within the active site of the kinase domian. (**b**) Solvent accesible surface area representation of PKCα focused on the active site of the kinase domain with wildtype p.D463 (Asp463) and bound ATP.

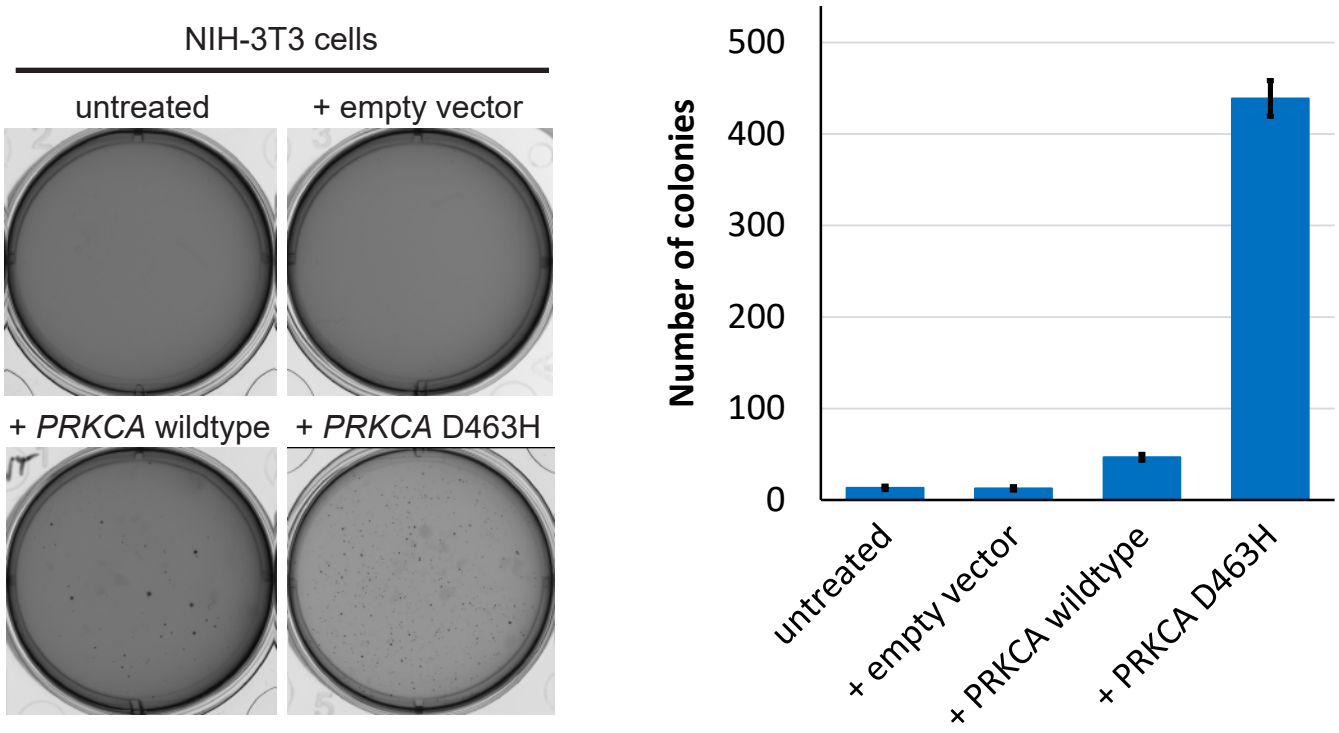

Supplementary Figure 8. Mutant *PRKCA* drives anchorage-independent growth of NIH-3T3 cells. NIH-3T3 cells were plated in soft agar 24 hours after lentiviral transduction with empty vector, wildtype *PRKCA*, or D463H-mutant *PRKCA*. Colonies were imaged and quantitated after 14 days. Error bars represent standard deviation from the mean of six replicates derived from two independent experiments performed in triplicate.

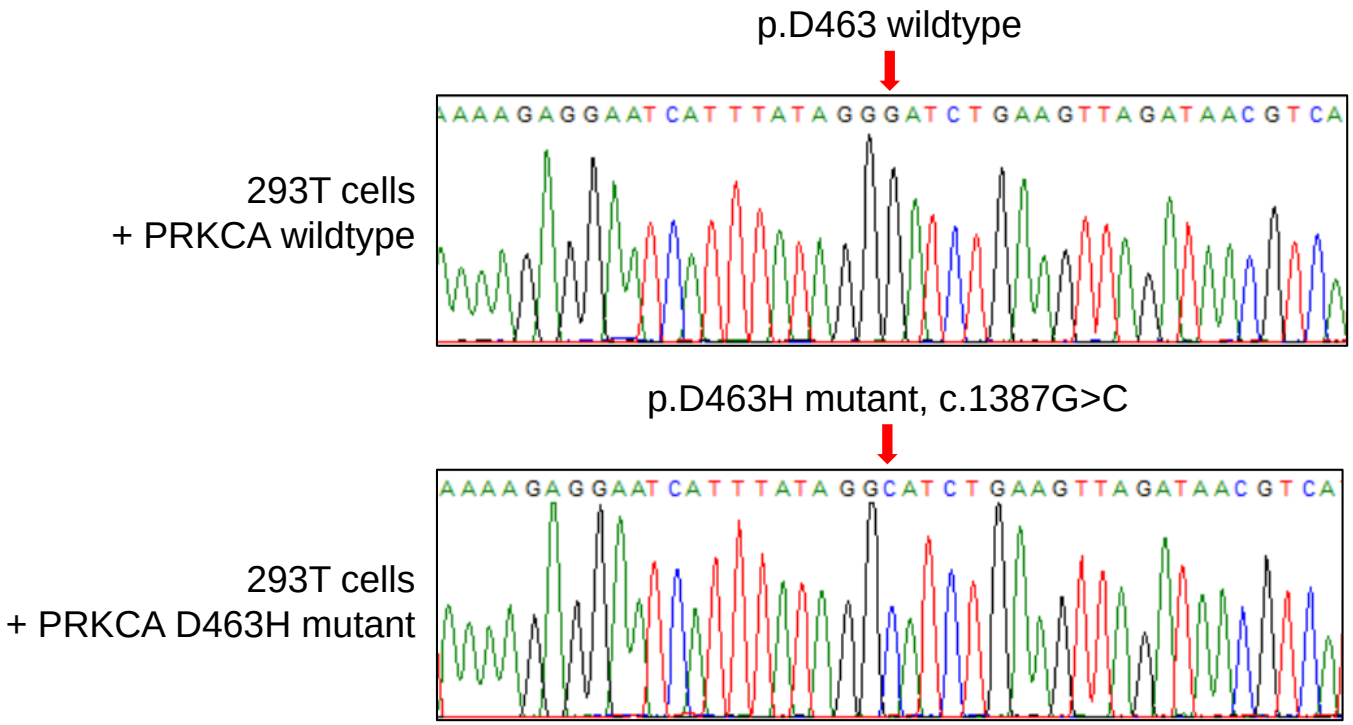

Supplementary Figure 9. Confirmation of wildtype and D463H mutant *PRKCA* mRNA expression after ectopic overexpression. Total RNA was isolated from 293T cells 48 hours after transient transfection with wildtype or D463H mutant *PRKCA* cDNA, and reverse transcription-PCR was performed to amplify *PRKCA* transcripts as described in the Methods. Shown are Sanger sequencing traces of these RT-PCR products.

from Figure 2b

phospho-ERK

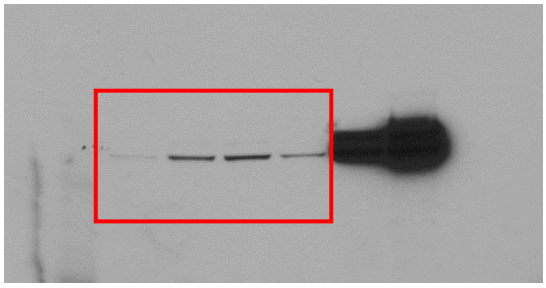

PKCα

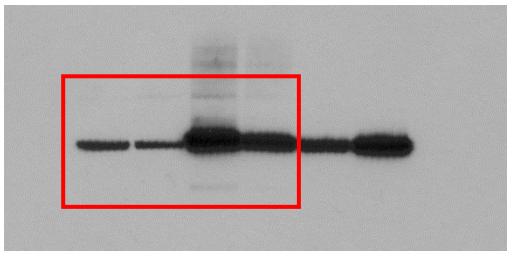

phospho-MARKCS

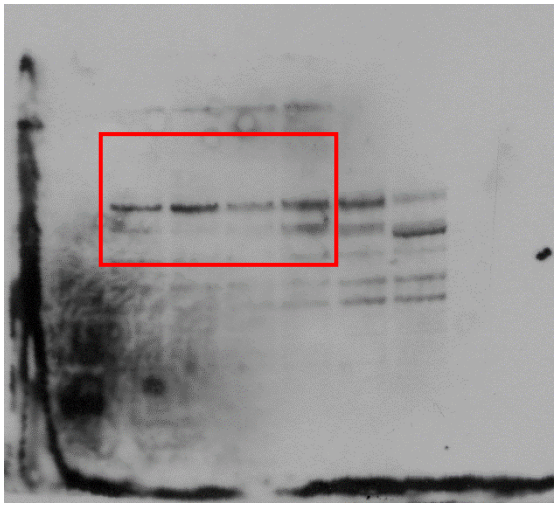

α-tubulin

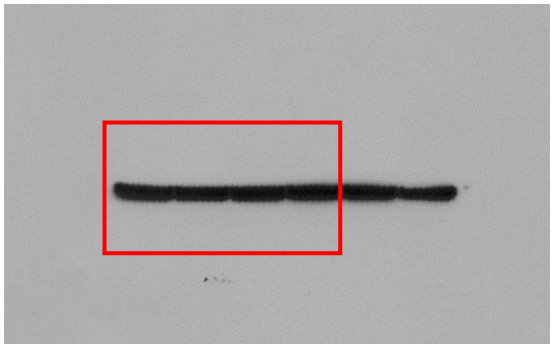

from Figure 2c

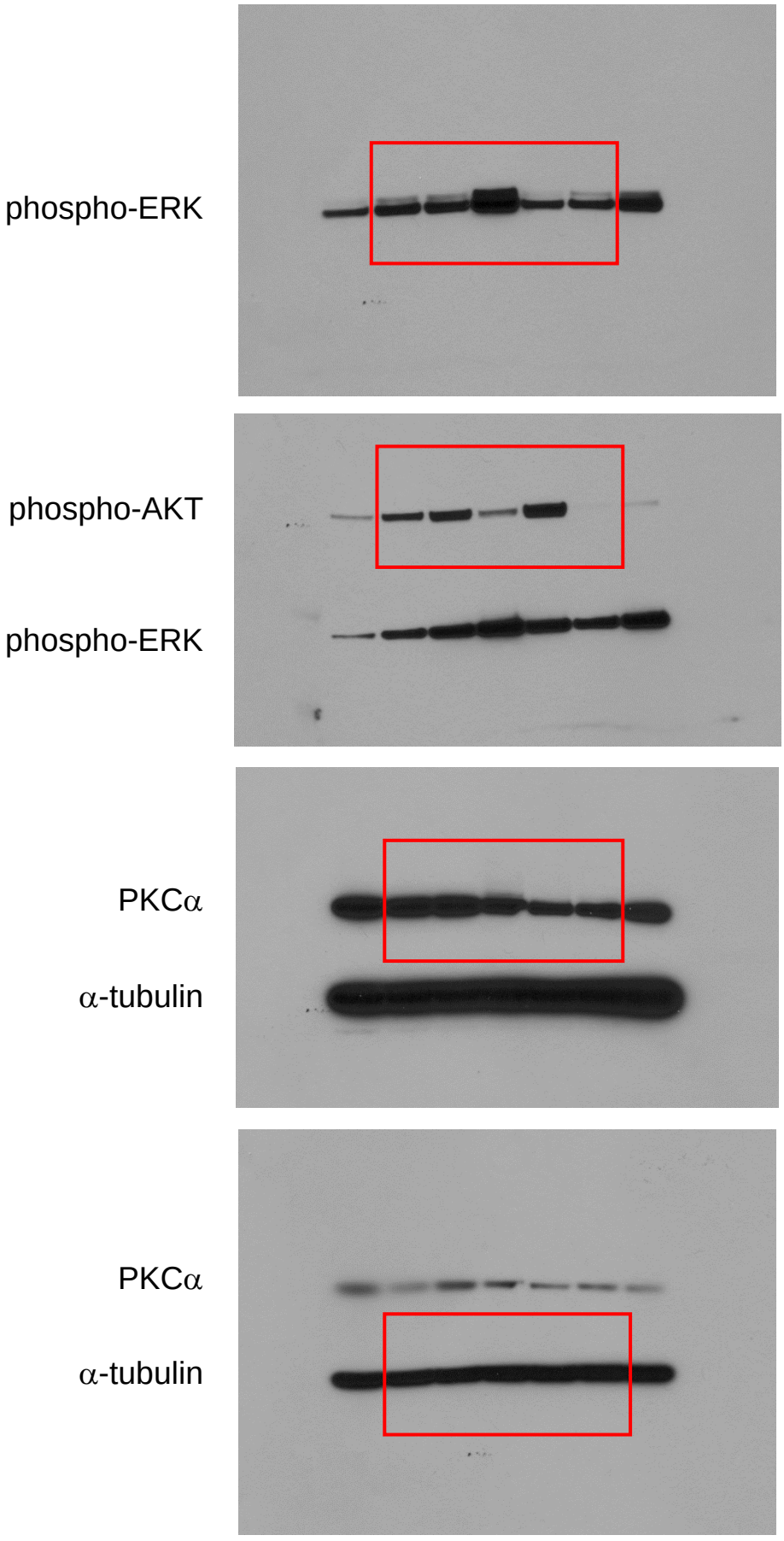

Supplementary Figure 10. Uncropped Western blots from Figure 2. The cropped region that is displayed in Figure 2b and 2c with sample labeling and molecular weight markers is highlighted in red for each blot.